Seawater Masses Characteristics of The Bali Sea Based on CTD Yo-Yo Casting

Gentio Harsono[1, 2*], Budi Purwanto[1], Rudy A.G Gultom[1], Tunggul Puliwarna[3], Johar Setiyadi[4], Kentaro Ando[5], Mario Cobral[6]

[1]*Faculty of Defence Technology, Republic Indonesia Defence University*
Kawasan IPSC Sentul, Sukahati, Kec. Citeureup, Bogor, Jawa Barat 16810 Indonesia
[2]*Hydro-Oceanographyc Center, Indonesian Navy*
Jl. Pantai Kuta V No. 1 Ancol Timur Jakarta 14430 Indonesia
[3]*Indonesian Naval Command and Staff College*
Jl. Ciledug Raya Cipulir Jakarta 12230 Indonesia
[4]*Indonesian Naval Technology College*
Jl. Pantai Kuta V No. 1 Ancol Timur Jakarta 14430 Indonesia
[5]*Japan Agency for Marine Earth-Science and Technology*
2-15 Natsushimachō, Yokosuka, Kanagawa 237-0061, Japan
[6]*Universidade Nacional Timor Lorosae*
Av. Cidade de Lisboa, Díli, Timor-Leste
Email: gentio.harsono@idu.ac.id

Abstract

The Bali Sea is located between the Java Sea and the Lombok Strait, which is one of the Indonesian Through Flow exits, especially the western route. These waters are possible to be the meeting place and mixing of two water masses with significantly different characteristics, that is the watermass brings by Indonesian Through Flow and Indian Ocean watermass. This study describes the watermasses and its turbulent mixture in the Bali Sea using CTD Yo-Yo casting data and spatial monsoonal wind distribution. The vertical distribution of energy dissipation rate and diapycnal diffusivity in the Bali Sea was computed based on measurement data during KRI RIGEL 933 expedition on April, 2021. KRI RIGEL is operated by Hidro-Oceanographyc Center Indonesian Navy's. Identified 4 types of water masses in a row, there are Java Sea water masses, mixed water masses between Java Sea and ITF, NPSW and NPIW with modified water mass property characters. The internal tides formed in the sills of the Lombok Strait are thought to contribute to the turbulent mixing parameters in the Bali Sea. The values obtained for energy dissipation and diapycnal diffusivity are 1.58 x 10^{-9} W Kg^{-1} and 5.07 x 10^{-5} m^2 s^{-1}, respectively. The value of this turbulent mixing parameter is confirmed to be smaller than the mixing value in the Lombok strait and is equivalent to the open sea. It is seen that there is a transformation of water mass which is marked by a shift in the density value in the identified water mass type.

Keywords*: Seawater Masses, Bali Sea, CTD Yo-Yo, Indonesian Through Flow, energy dissipation*

Introduction

Indonesia, which has a complex and narrow topography as the only channel of water mass exchange from the tropical waters of the Pacific Ocean to the Indian Ocean, or better known as the Indonesian Traffic Stream (Gordon and Fine, 1996; Sprintall *et al*., 2004). The Indonesian Through Flow (ITF) as formed due to a push due to the difference in sea level between the Pacific and Indian Oceans (Susanto and Song, 2015; Sprintall *et al*., 2019) this difference reached an average of ±20 cm (Mayer and Damm, 2012). The ITF has two routes, the western route which enters through the Celebes Sea and then to the Makassar Strait, Flores Sea, and to the Banda Sea. The second route is the eastern route which passes through the Maluku Sea and the Halmahera Sea and then to the Banda Sea (Fieux *et al*., 1996). The ITF carries water masses of NPSW and NPIW on the western line and SPSW and SPIW on the eastern route to the Indian Ocean through Indonesian waters (Fine *et al*., 1994; Wyrtki, 1961). The thermocline layer (NPSW/SPSW) is centered on isopycnal 24-24.5 with maximum salinity characteristics and intermediate layer (NPIW/SPIW) and centered on isopycnal 25-26.5 with minimum Salinity characteristics (Kashino *et al*., 1996; Atmadipoera *et al*., 2009; Kashino *et al*., 2009).

A lot of research on ITF has been carried out on the west and east routes, mainly on the inlet routes, such as the Makassar Strait and the Lyfamatola Canal and the exit routes, such as the Lombok Strait, Ombai Strait, and the Timor route (Arief and Murray,

*) Corresponding author

https://ejournal.undip.ac.id/index.php/ijms
DOI: 10.14710/ik.ijms.26.4.282-297
Received : 15-09-2021
Accepted : 03-11-2021

1996; Gordon *et al*., 2010; Molcard *et al*., 2001; Susanto and Gordon, 2005; Sprintall *et al*., 2009; van Aken *et al*., 2009; Wang *et al*., 2020). Including ITF secondary pathways that enter from the Karimata strait and exit through the Sunda strait (Fang *et al*., 2010; Susanto *et al*., 2016; Wang *et al*., 2019). ITF through Indonesian Seas experienced changes in temperature and salinity characteristics due to turbulent mixing. Research on turbulent mixing related to the value of energy dissipation and diapycnal diffusivity has been carried out based on numerical models and direct observations on the west and east lines. The area includes narrow and localized straits such as the Lombok Strait, Ombai Strait, Lifamatola Strait, Alor Strait (Adhyatma *et al*., 2019; Purwandana *et al*., 2014; Suteja *et al*., 2015; Nagai *et al*., 2017). In addition, in wider water areas such as in the Dewakang waters, the Labani canal, the Banda Sea, the Sulawesi Sea, the Makassar Strait (Koch-Larrouy *et al*., 2010; Nagai and Hibiya, 2015, Purwandana *et al*. 2020, Nagai *et al*., 2015; 2021). However, none of these studies directly estimate the value of turbulent mixing in the Bali Strait, which is directly adjacent to the Lombok Strait, which is the exit route for the ITF, and the Java Sea, which has very contrasting characteristics with the ITF.

This study presents measurements of temperature and salinity values as material for calculating turbulent mixing in the Bali Sea. The Bali Sea is the waters located between the Java Sea and the Flores Sea and between the Lombok Strait and the Bali Strait. The Bali Sea is a water that is quite unique because it is like a cup. In the west it is bordered by the island of Madura which has fairly shallow waters and the Bali Sea in some areas has waters that are deep enough to reach more than 1000m. Its location is close to the lombok strait, where the lombok strait is one of the waters in Indonesia where internal waves are formed as conversion of barotropic tides to baroclinic which has been observed directly, numerical models or using satellites (Hatayama, 2004; Schiller, 2004; Robertson and Ffield, 2005; Koch-Larrouy *et al*., 2007; Karang *et al*., 2012; Ray and Susanto, 2016; Bouruet-Aubertot *et al*., 2018; Nugroho *et al*., 2018).

This makes the sea water mass of Bali have the potential to be influenced by the internal waves phenomenon. The main purpose of the field measurements carried out by Pushidrosal is to understand and describe the oceanographic conditions in the Bali Sea. It use these newly acquired data to fill the research gaps between the needs of an updated data and the best available data from historical cruise surveys and previous studies. This study presents the dynamics of the waters, their relationship with the ITF and the Java Sea and its influence factors.

Materials and Methods

Data acquisition

Field observations in this study were carried out using KRI Rigel 933 is operated by Hydro-oceanography Center Indonesian Navy's (PUSHIDROSAL) on April 30, 2021. The research location is in the Bali Sea which neighbouring with Java Sea in the west, the Flores Sea in the north, the Kangean Islands in the north and the island of Bali to the south. In addition, this location is also between the Bali Strait and the Lombok Strait with the bounding area coordinates between 6.5°- 9.5° South Latitude and 113.5°-116.5° East Longitude (Figure 1.).

A total of 8 replicates were obtained in a 12-hour data collection period (Figure 2.). The accuracy and resolution of temperature sensors are 0.01°C and 0.005°C, respectively, with a temperature range of -5°C to 35°C, and for conductivity sensors are 0.01 mS.cm^{-1} and 0.003 mS.cm^{-1}, respectively. The processed data only comes from downcast data, namely profile measurements when the CTD is lowered into the waters. After the data pre-processing stage is done, then the data is corrected manually such as removing noise and spikes. The data pre-processing stage was carried out as done by McTaggart *et al*. (2010).

Three stations of tidal data i.e in the Indan Ocean, Lombok Strait and Bali Sea which obtained from the Geospatial Information Agency (BIG) (http://tides.big.go.id) are used as secondary data to supports the analysis. Temporal resolution of tidal data is hourly during 24 h in 6 days observation. Wind data is taken from ECMWF Era-5 (https://www.ecmwf.int/), while ocean current data is taken from marine copernicus (https://marine.copernicus.eu/). Both wind and ocean current directional are in zonal (U) and meridional (V) format components. hourly ocean currents and wind data over a 12 h period adjusted for CTD data recording. Wind and ocean current data are employed to investigate the sea-air interaction in the surface layer of seawater mass. Sentinel-1 satellite imagery was obtained from https://sentinels.copernicus.eu/ with observations on the same day and time as yo-yo CTD data collection.

Turbulent mixing analysis

Thorpe's displacement is very useful for describing the vertical range of mixing events. Thorpe is determined from the density repetition in the form of static stability according to the initial density or depth. The first step is to determine Thorpe

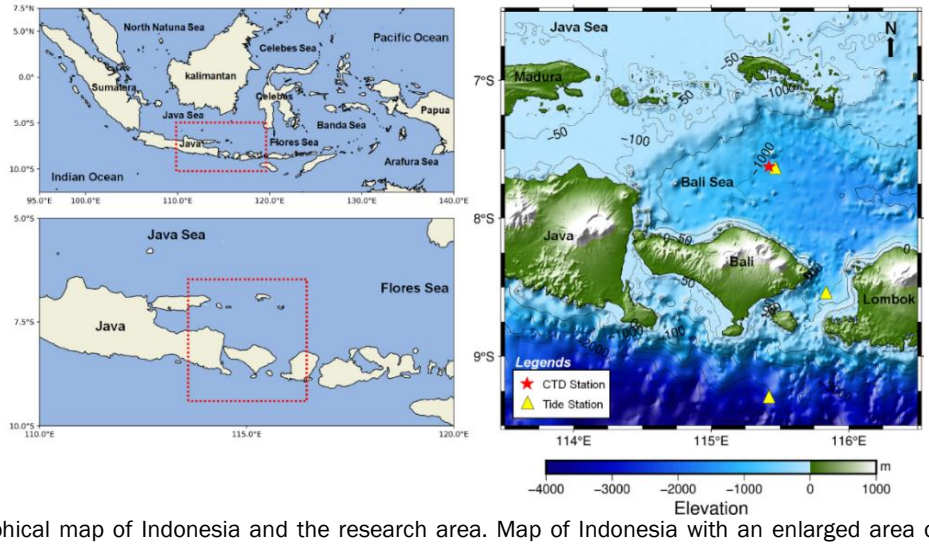

Figure 1. Geographical map of Indonesia and the research area. Map of Indonesia with an enlarged area of Java and Nusa Tenggara (top left). Map of Java-Nusa Tenggara with magnification of the research site (bottom left). Map of the research location with a red star as the location for CTD data collection and a yellow triangle for tidal observation points. (Maps created in python 3.8.5 https://www.python.org/downloads/release/python-385/ with jupyter notebook IDE)

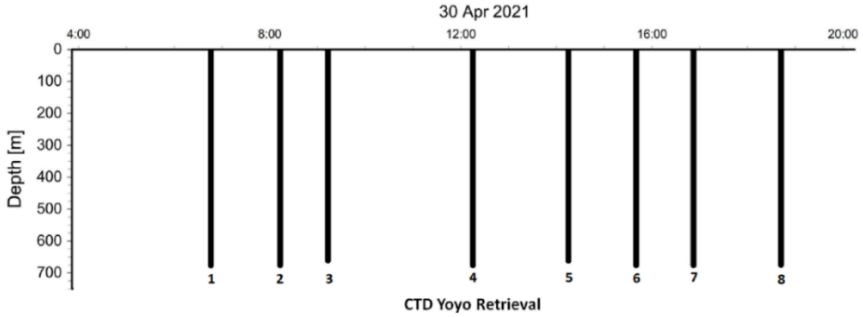

Figure 2. Collecting CTD data using the yo-yo method in the Bali Sea. Data collection was repeated 8 times with a period of 12 h from 7 to 18 local time with various depths in the range of 680m.

Displacement (Td) (Dillon, 1982):$Td = za - zb$. The identified Td was validated by the water mass test of Galbraith and Kelly (1996) which is commonly called the GK test. The threshold used is 0.7 to minimize the GK test rejecting some real overturns which are usually small overturn areas (Stanfield *et al*. 2001). The calculation of the amount of kinetic energy undergoing the dissipation process based on the Ozmidov scale is: $\varepsilon = L_o^2 N^3$ and the turbulent diapycnal diffusivity value at each depth is then obtained by applying: $K_z = \frac{\gamma\varepsilon}{N^2}$ by Osborn (1980) with the value of γ = 0.2 which has been confirmed by empirical calculations by Purwandana *et al*. (2020) and N are Brunt Vaisala frequencies. The results obtained will be averaged every 50m and will be displayed to a depth of 650m. The final result shows the mean and standard deviation of all CTD Yo- Yo replicates in the Bali Sea. Stratification of water column layers based on temperature variations using a temperature threshold (ΔT) or using a gradient. In this study the criteria used were based on gradients. Hao *et al*. (2012) stated that the thermocline layer can be identified by using temperature gradient is >0.05^{o}C.m^{-1}. Analysis of water mass characteristics using TS (Temperature-Salinity) can be used also to study the mixing of water masses (Emery and Thomson, 1998). TS-diagram is employed to identify the seawater mass types and its origin, refers to Wyrtki (1961) classification.

Result and discussion

Hydrography structure

Determination of water column layer stratification based on temperature gradient (ΔT) by Hao *et al*. (2012). The results of the determination of layer stratification can be seen in Figure 3. Mixed layers are characterized as a uniform layer with small changes of temperature, salinity, and density to the depth. One of the factors that cause mixing in the surface layer is wind friction. This wind dynamic causes the temperature to be relatively homogeneous. In addition, the mixed layer has a high temperature value because it is in a surface layer that is directly receiving solar radiation (Steward, 2002).

The thermocline layer is between the mixed layer and the inner layer with the most significant decrease in temperature values. The upper limit of the thermocline layer has appear in 44m depth and the lower limit is founded in 233m depth. It is clear that the increase in water mass property in the thermocline layer is clearly visible. The thermocline layer gives a greater response to the internal wave than other layers (Susanto *et al*., 2005). The inner layer is below the thermocline layer with the characteristics of insignificant changes in temperature, salinity and density and tends to be homogeneous.

The values of physical parameters (temperature, salinity and density) can be seen in Figure 4. The temperature at the upper limit has a more uniform value than the lower limit. The mixed layer has a more homogeneous value because the dynamics on the surface of the water are large enough to cause greater mixing The salinity in Bali Sea has more variations, since it constructs by the fresher Java Seawater mass and saltier ITF seawater mass from Makassar Strait, and also form Indian Ocean seawater mass from Lombok Strait. The role of temperature and salinity in these waters affects the density value. The upper limit of the role of salinity is more dominant, while the lower limit of the influence of salinity and temperature is equally dominant.

Figure 5 shows the cross-sectional distribution of temperature, salinity, and density from sea level to the last data 680m. The distribution pattern of these three parameters still leaves a tidal pattern although it is not significantly visible. This tidal pattern can still be seen quite clearly in the thermocline layer, indicated by a downward pattern on the isothermal line 20 when the tide enters the receding phase. It is also seen that the core of high salinity in the thermocline layer also follows the tidal pattern. The high-salinity core in the thermocline layer decreases deeper when the tide is in the receding phase. Tidal patterns that interact in these waters originate from the Lombok Strait which is located in the southeast of the Bali Sea (data collection location). The distribution pattern following the tidal pattern begins to weaken at a depth of 300m. The structure of the layering of physical parameters in the Bali Sea is generally well stratified and below 300m the vertical gradient begins to weaken.

To investigating the distribution of salinity-temperature and the character of the mass of water in the the Bali Sea, a TS diagram has been plotted (Figure 6.). The water mass in the Bali Sea comes from the North Pacific Ocean (Hautala *et al*., 1996, Ffield and Gordon, 1992, 1996) in the thermocline and sub-thermocline (intermediate) layers, while the Java Sea in the surface layer. The mass of Java Sea water that is on the surface because it has a low density because it is composed of fresh salinity and colder water mass temperature.

The mass of Java sea water reaches the waters of the Bali Sea because of the flow from the South China Sea which enters from the Karimata Strait and then into the Java Sea (Gordon *et al.*, 2010). Right between the Java Sea water masses, there is a mixed water mass between the Java Sea and the ITF west route that exits through the Lombok Strait. Siregar *et al*. (2017) in his research found that the seasonal average salinity during the east

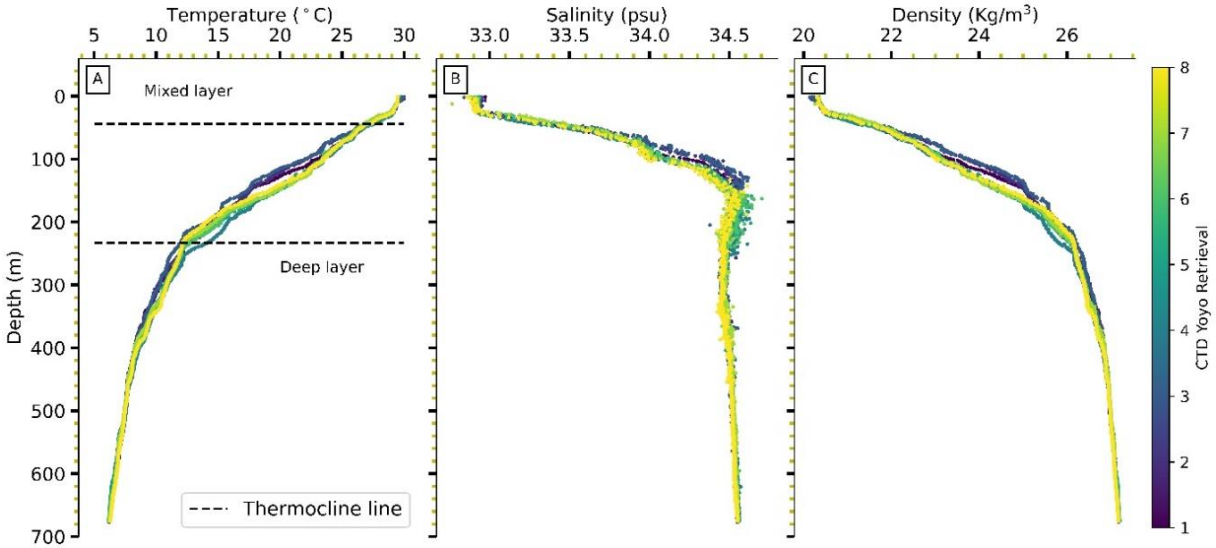

Figure 3. A vertical graph of physical parameters with color gradations according to the time of retrieval represented by the CTD yo-yo retrieval number. Respectively for the parameters (A) Temperature, (B) Salinity and (C) Density. The black dotted line is the boundary line of the thermocline layer

monsoon was higher (31-34 psu) than the west monsoon (29.5-33 psu), and the temperature during the east monsoon was lower (27-30.5°C) compared to the western monsoon (28.5-30.5°C). Arlindo strengthens during the east monsoon and weakens during the west monsoon. In the west monsoon, the Java Sea is filled by the water mass of the South China Sea, while in the east monsoon which coincides with the Arlindo phenomenon, the water mass of the Java Sea is filled by the water mass of the Makassar Strait. while in the transitional monsoon the Java Sea is filled by the water mass of the South China Sea and also the Makassar Strait. This water mass was later identified in the Bali Sea. This mass of water fills the water column between the Java Sea and the ITF, which is quite visible with the presence of diapycnal mixing which is indicated by changes in water mass properties (salinity and temperature) crossing the isopycnal line.

The core layer of water mass with maximum salinity at a depth of 150 m is known as North Pacific Subtropical Water (NPSW) while the core layer S min at a depth of 300 m is North Pacific Intermediate Water (NPIW). Both entered Indonesian waters through the ITF western route and experienced changes in characteristics (temperature and salinity) when passing through Indonesian waters due to the complex dynamics of the waters. The complete characteristics of the water masses that have been identified can be seen in Table 1. The probability of temperature, salinity and density for each mass of water can be seen in Figure 7. It is clear that there is a change in the characteristics of the core of the water mass. The NPSW water mass undergoes a change in density core. Previous studies have identified NPSW in the isopycnal range from 24–24.5 kg.m^{-3} (Atmadipoera *et al*., 2009; Kashino *et al*., 1996). This study found the mass of NPSW water in the isopycnal range of 24.6–25.4 kg.m^{-3} which was concentrated at 25.1 kg.m^{-3}. Still in comparison to previous studies, this study found that the NPIW experienced an increase in the density value in the range of 26.4 – 26.7 kg.m^{-3}, although it was still with the same value range, the previous study was 25–26.5 kg.m^{-3}. The displacement of the core values in isopycnal is a strong indication of the transformation water mass due to turbulent mixing in the waters. The peaks of the distribution of values for each parameter are the core characteristics of the water mass in the waters of the Bali Sea.

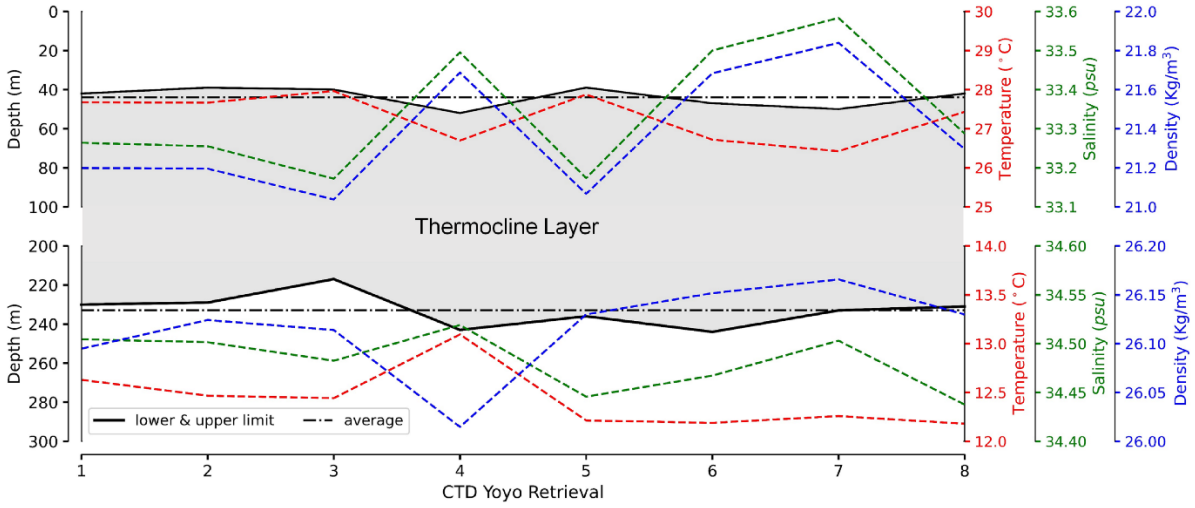

Figure 4. The stratification profile of the Bali Sea layer at the time of yo-yo CTD measurement. The thermocline layer between the upper and lower limits is gray. The upper and lower boundaries bordering the homogeneous layer are solid black lines and black dots for the average value. The dotted lines are for values that are at the layer boundary, respectively for the red color temperature, green color salinity and blue color density.

Tabel 1. Characteristics of the mass of seawater in Bali

Type	Depth [m]	Temperature [°C]	Salinity [psu]	Density [kg.m-3]
java Sea	1 - 41	27.87 - 29.99	32.76 - 33.19	20.13 - 21.07
java Sea - ITF	47 - 112	22.88 - 26.65	33.49 - 34.22	21.70 - 23.37
NPSW	122 - 197	15.60 - 19.69	34.53 - 34.7	24.55 - 25.54
NPIW	261 - 387	8.87 - 11.46	34.42 - 34.49	26.26 - 26.72

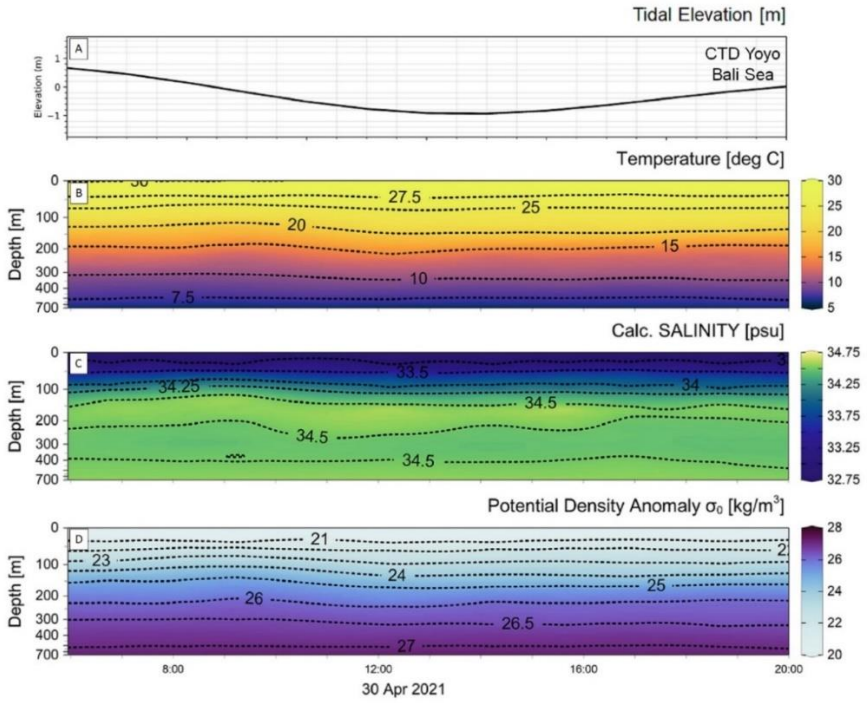

Figure 5. (A) Tidal elevation chart during the Yoyo CTD data collection period. Transverse profile to depth during the Yoyo CTD data collection period for (A) Temperature, (B) Salinity and (C) Density.

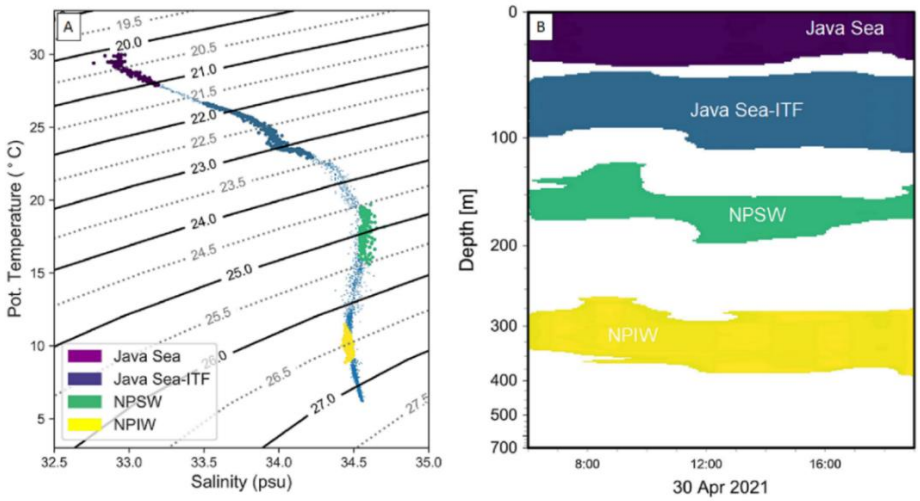

Figure 6. Identification of water masses in the waters of the Bali strait. (A) TS Diagram with description of the type of water mass, purple Java sea, blue Java sea-ITF, green NPSW and yellow NPIW. (B) Position with respect to the depth of the water mass identified in the Bali Sea. The color of each type of water mass is in accordance with the TS Diagram image.

Turbulent mixing analysis

The existence of instability in the water column has the potential to trigger a mixture of water masses. This can be expressed by calculating the value of the buoyancy frequency or the Brunt Vaisala frequency. The results of the calculation of the Brunt Vaisala (N2) frequency from the overall CTD yo-yo sampling can be seen in Figure 8 (red). It can be seen that the value of N2 experienced a significant increase when it entered the thermocline layer (pycnocline). The thermocline layer in this study was found to coincide with the pycnocline layer (Figure 3.). This pattern is similar to that obtained by Guo *et al*. (2006) in the northern South China Sea. The high value of N2 in the thermocline layer is because in this layer the density gradient increases significantly with depth (pressure). The thermocline layer can be interpreted as the most stable layer compared to the mixed surface layer and the inner layer. If the value of N2 is higher, the static

stability of a layer will be greater. In each repetition of Yoyo's CTD retrieval, the value of N2 was quite high and constant in the thermocline layer. This high N2 value condition begins to appear in the range of 40m and persists to a depth of 210m. then below 210m the value tends to be small and slopes to the last data or depth when entering the deep layer.

The density inversion distribution in this study uses data from CTD to evaluate the mixing conditions in the water column. The relationship between density inversion and turbulent mixing is closely related and has been discussed in detail by (Thorpe 1977; Dillon 1982; Crawford 1986). The vertical density profile obtained from CTD measurements has a water mass instability structure that can be seen from the Brunt Vaisala frequency value that has been obtained. Displacement of a water mass parcel due to the presence of a water mass parcel having a high density value above a water mass parcel having a lower density in an area of water can occur. Figure 8 (blue) visualizes the unstable condition of the water mass is representing a Thorpe displacement. Thorpe displacement is obtained from the comparison of the measured density value with the density that has been rearranged. Thorpe displacement values observed in this study showed a significant difference between the thermocline layer and other layers. The Thorpe displacement value in the thermocline layer in all replicates of Yoyo CTD sampling shows a relatively small value because the thermocline layer is a stable layer.

Based on the estimation of mixing using the Thorpe method, the range of energy dissipation and diapycnal diffusivity values in Bali Sea waters is obtained. This range of energy dissipation and diapycnal diffusivity values was obtained from the average every 50m on all repetitions of Yoyo CTD data collection. The energy dissipation and diapycnal diffusivity values can be seen in Figure 9. In this study, the range of energy dissipation and vertical diffusivity values was O (Ordo) 10^{-8} - 10^{-11} W Kg^{-1} and O 10^{-4} - 10^{-7} m2 s^{-1}. The distribution of energy dissipation values at depth has a fairly large range value. The largest range of energy dissipation values is around the surface and the highest in the thermocline layer. The range of energy dissipation values successively decreases with increasing depth. The diapycnal diffusivity range has a similar pattern to energy dissipation but with a different range.

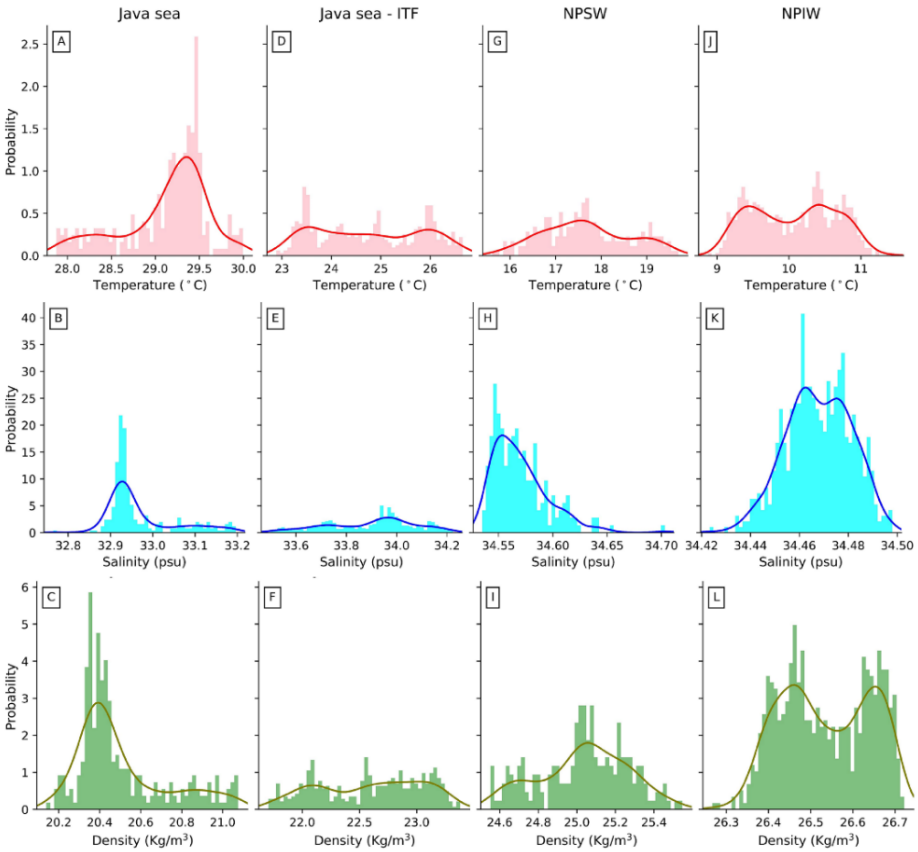

Figure 7. Probability of water mass characteristics based on the identified water mass type. The characteristics of the water mass in the form of salinity, temperature and density respectively (A), (B) and (C) for the Java sea water mass. (D), (E), and (F) for JS – ITF. (G), (H), and (I) for NPSW water masses. (J), (K), and (L) for the mass of NPIW water.

Starting at a depth of 450m the range of energy dissipation values decreases significantly and finally starting at a depth of 500m the value range is close to 0 10^{-10} - 10^{-11} W.kg^{-1}. The range of diapycnal diffusivity values decreases with increasing depth. The range of diffusivity values on the surface to a depth of 450m has a value that is quite close in the range of 0 10^{-4} - 10^{-6} m^2 s^{-1}. It can be seen that there is a significant difference when it reaches a depth of 500m, there is a spike in the value reaching 0 10^{-1} m^2 s^{-1} until the value shifts smaller in the range of 0 10^{-5} - 10^{-7} m^2 s^{-1}. The results obtained are not much different from the research conducted by Munk (1966) with the assumption of a balance of advection and diffusion to obtain an average global diapicnal diffusivity value with Kz 10^{-4} m^2 s^{-1}. More specifically, Gregg (1998) and Polzin *et al*., (1995) in their research obtained diapycnal diffusivity values of Kz 10^{-6} m^2 s^{-1} and Kz 10^{-5} m^2 s^{-1}. The diffusivity value in the Bali Sea is equivalent to the open sea, significantly different from the nearby waters, namely the Lombok Strait, which has a rough water topography. Water areas with high mixed values are found above the rough topography (Ledwell *et al*., 2000; Wu *et al*., 2011).

The average value and standard deviation of energy dissipation and diapycnal diffusivity can be seen in Figure 10. The average value of energy dissipation in all replicates of yo-yo CTD data collection and to depth is 1.58x10^{-9} W kg^{-1} and the vertical diffusivity value is 5.07x10^{-5} m^2 s^{-1}. The value obtained is small and identical to the value of the open ocean when compared to the large value in the Lombok strait. The Lombok Strait which is adjacent to the Bali Sea is able to achieve energi dissipation value

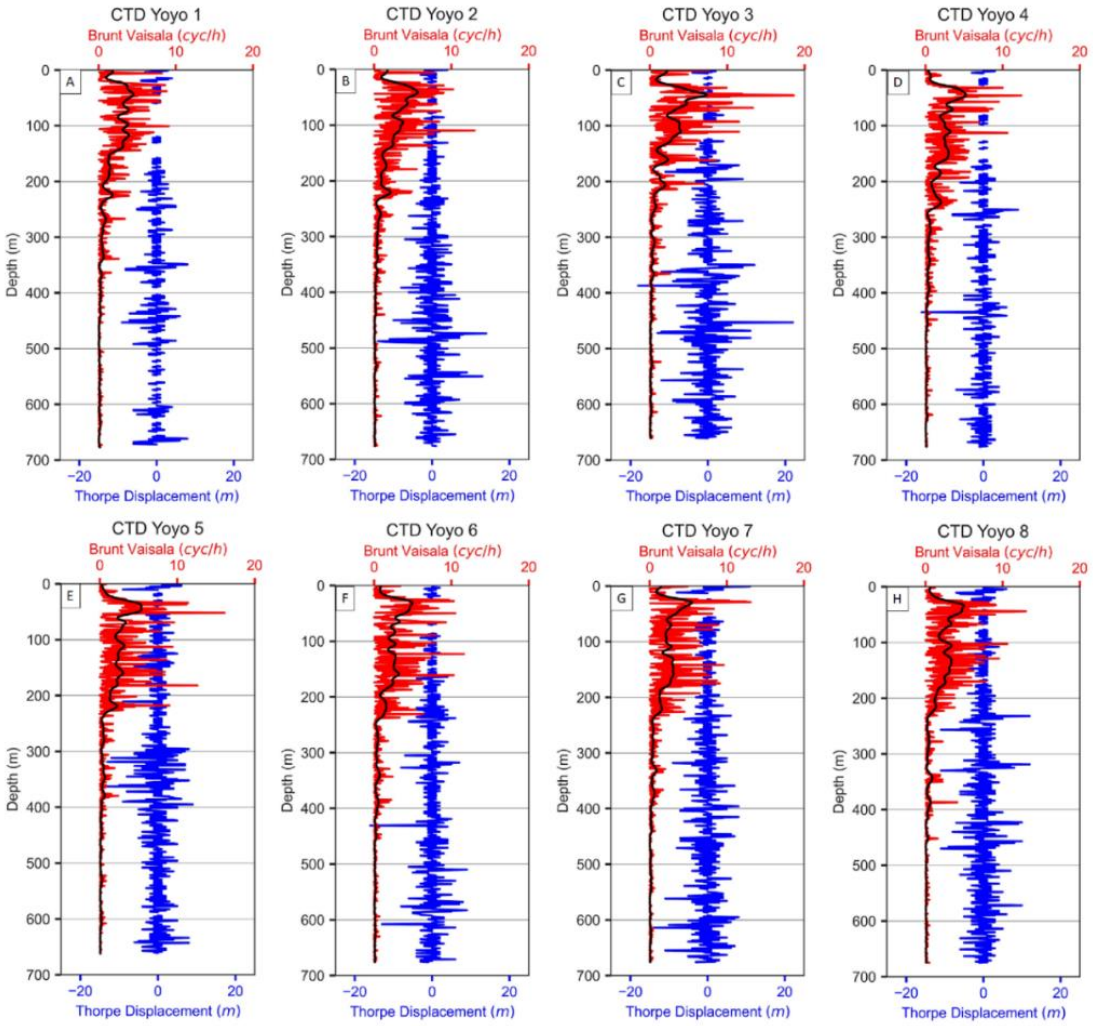

Figure 8. Vertical graph of Brunt Vaisala value (red) with smooth fit (black) and Thorpe displacement (blue). Figures (A), (B), (C), (D), (E), (F), (G) and (H) are for CTD Yoyo 1, 2, 3, 4, 5, 6, 7 and 8 respectively, with the same Brunt Vaisala scale and Thorpe displacement.

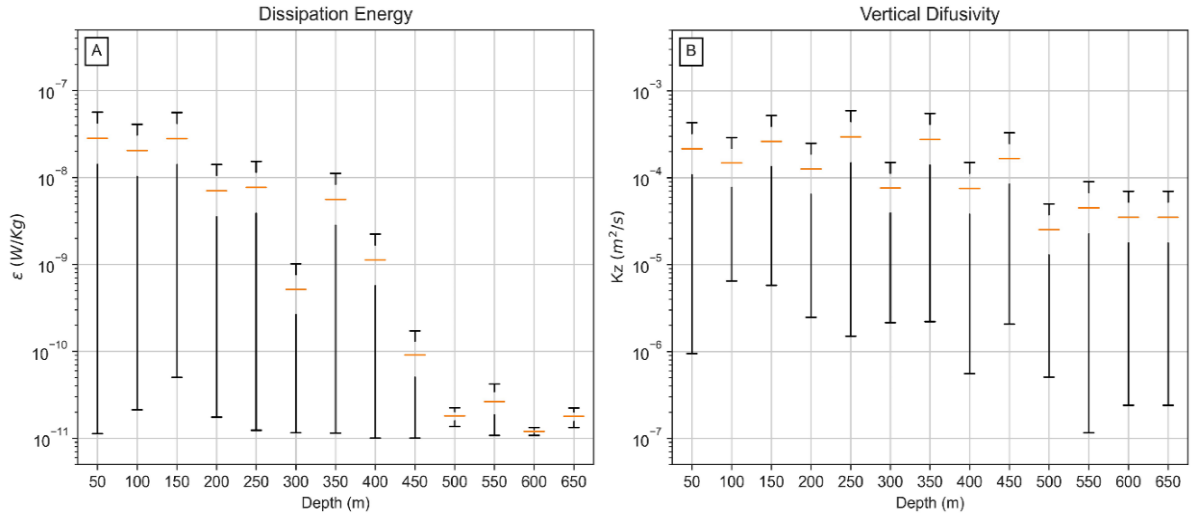

Figure 9. Graph of the range of values of (A) energy dissipation and (B) diapycnal diffusivity based on the average results of all Yoyo CTD retrieval data with the orange line being the average value.

of 0 10^{-5} W kg^{-1} and diapycnal diffusivity at 0 10^{-2} m^2 s^{-1} in the study of Purwandana *et al*. (2020); Nagai *et al*. (2021); Yuliardi *et al*. (2021). The high value of turbulent mixing is not only correlated with topography but also with shear which encourages the dissipation process. ITF flow in the thermocline layer causes the energy dissipation value in the thermocline layer to be greater than in other layers. Turbulent mixing in the thermocline layer can be driven by various factors, including surface winds, internal waves, and internal tides.

Dynamics of the ocean and atmosphere

Figure 11 presents a plot of wind flow at the time of yo-yo CTD data collection. The wind moves in a dominant direction from southeast to northwest. Indonesia's territory, which is located at the equator and between the continents of Asia and Australia, makes Indonesia's climate strongly influenced by the six-month monsoon system (Aldrian and Susanto, 2003). It can be seen that the maximum wind speed is in the ocean and weakens when it reaches land. This is because the topographic contours of the land are uneven and in the areas of Nusa Tenggara, Bali and East Java, there are high mountains that are able to reduce wind speed.

The wind that blows affects the flow of the upper layer currents in the Bali Sea, especially in the strait area due to intensification (Figure 12.). This pattern appears mainly during the summer (southeast monsoon) from April to October. When the wind blows from the southeast to the northwest, the wind will align with the islands in the archipelago chain of Nusa Tenggara and Java. This will trigger upwelling because the water mass is pushed away from the land. There is a water mass vacancy that causes lower sea levels throughout Nusa Tenggara and Java (Wyrtki, 1987). In addition, this will cause a pressure gradient between the northern and southern regions so that it will increase the intensity of the ITF flow (Wirasatriya *et al*., 2020).

The tidal dynamics can be seen in Figure 13. It is clear that the difference in tidal elevation is quite significant during the data acquisition area. The highest tidal elevation is at the point of the Indian Ocean. Indonesia is dominated by the M2 tidal component which propagates from its starting point in the Indian Ocean and enters Indonesian waters and one of the gates is the Lombok Strait (Robertson and Ffield, 2005). The Lombok strait has significant harmonic components such as the O1 component in the diurnal type, the semi-diurnal type has M2, the long period has SA, SSA, MSF components and in shallow waters the M6 significant harmonic component is obtained. The influence of internal waves based on SNR (Significant Noise to Ratio) is the harmonic components M4, MS4, MSF and O1 (Pratomo *et al*., 2016). The tide enters the Lombok Strait with significantly different elevations due to the presence of a sill at the southern end of the Lombok Strait. This reduced tidal elevation leads to the conversion of tidal energy from barotropic to baroclinic and into internal tides which are then known as internal waves which have the same period as the tide (Koch-Larrouy *et al*., 2007).

This study found that during yo-yo CTD data collection it was clearly seen that there were internal wave propagation from the Sentinel-1 satellite observation. Pratomo *et. Al.* (2016) stated that at a depth of 350 meters and 450 meters there was an

interesting current pattern, the speed and direction of the current tended to be north-northeast and south-southwest. This is due to the influence of Arlindo and the influence of long waves from the Indian Ocean that enter the Lombok Strait. These long waves form an internal wave when they pass through the sill as their propagation enters the Lombok strait. This internal wave propagation spreads from the place of its formation in the Lombok Strait towards the southwest, close to the Kangean Islands (Figure 14).

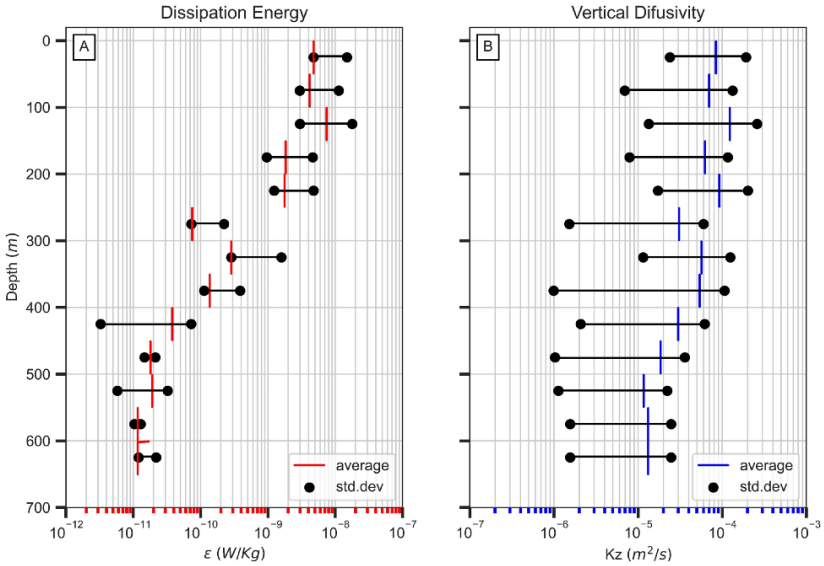

Figure 10. (A) average value of energy dissipation (red) and (B) average diapycnal diffusivity value (blue) with a range of standard deviation values (black dots) connected by black lines.

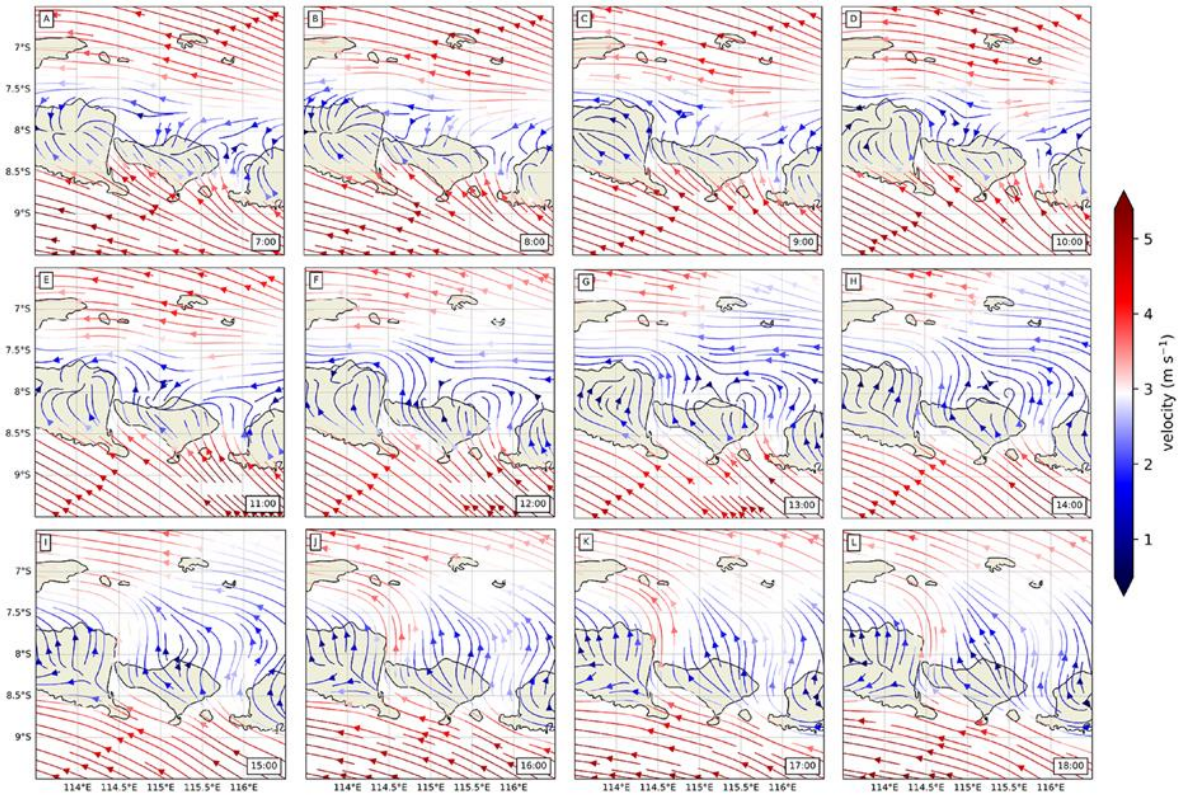

Figure 11. Profile of the flow direction and wind speed in the data collection period (12 hours). Figures (A), (B), (C), (D), (E), (F), (G), (H), (I), (J), (K) and (L) respectively. respectively for wind data snippets at 07:00, 08:00, 09:00, 10:00, 11:00, 12:00, 13:00, 14:00, 15:00, 16:00, 17:00, 18:00 with the same velocity bar scale.

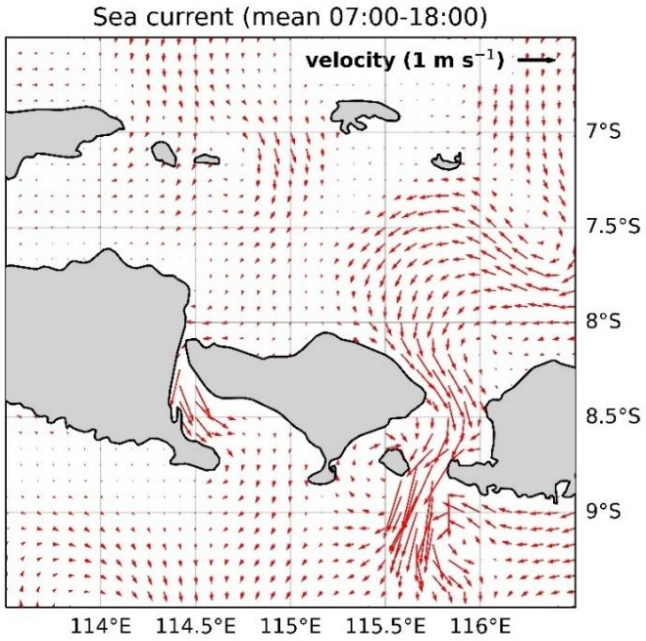

Figure 12. Profile of flow direction and average sea surface current velocity over a 12-hour period of yo-yo CTD data collection.

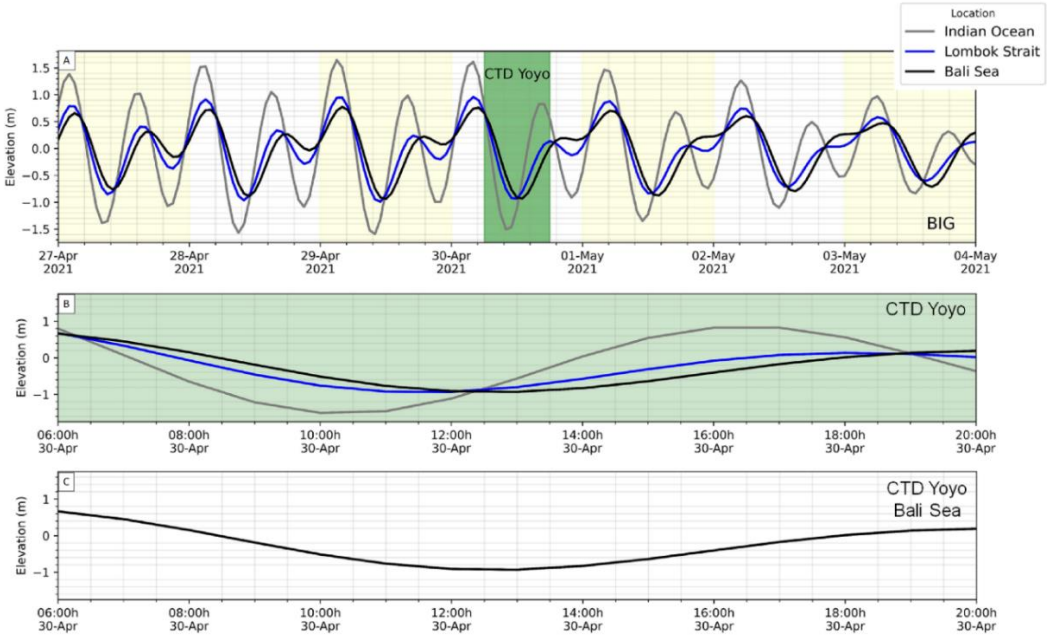

Figure 13. (A) comparison of tidal elevations in three areas with a span of one week. The Indian Ocean region is gray, the Lombok Strait is blue and the Bali Sea is black. Highlight the green color for the time marker and tidal elevation when taking CTD Yoyo. Highlight in yellow for the daily limit. (B) zoom period when the Yoyo CTD is taken. (C) tidal elevation during CTD Yoyo collection in the Bali Sea.

The mass flow of water in the Lombok Strait is influenced by the presence of a sill as a specific place for the formation of internal waves between the islands of Nusa Penida and the island of Lombok with a depth of up to 350m (Murray and Arief, 1988). Research on internal waves in the Lombok strait has previously been carried out using numerical models (Aiki *et al*., 2011), satellite observations (Karang *et al*., 2012), observations using Coastal Acoustic Tomography (CAT) (Syamsudin *et al*., 2019) and high-frequency comprehensive observation (Purwandana *et al*., 2021).

Previous studies have found that this strait is one of the straits with a very active internal wave generation and the internal waves formed develop

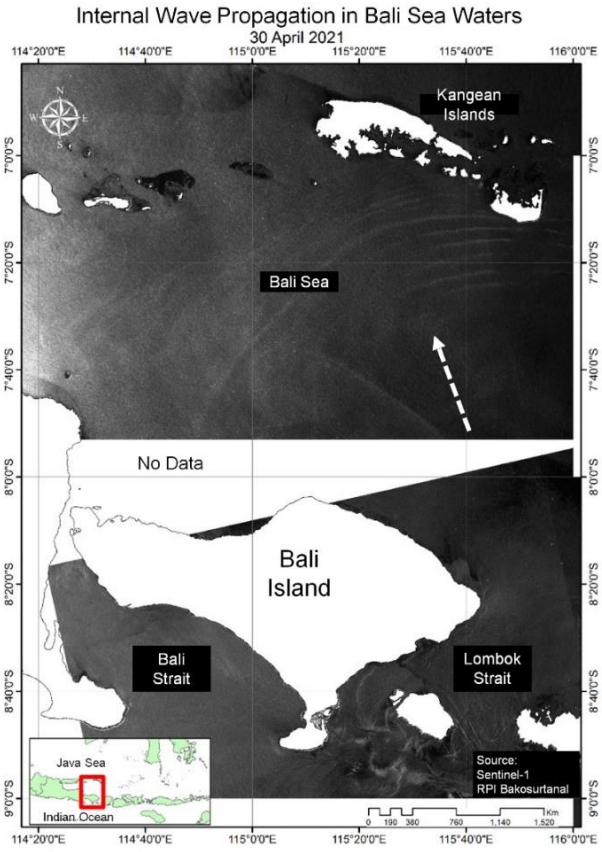

Figure 14. Internal waves in the bali sea by Sentinel-1 at 15:00 local time. The white dotted line shows the direction of propagation from its formation in the Lombok Strait to the Kangean Islands. The map inset at the bottom left with a red box shows the observation location covering the area around the waters of the Bali Sea.

into solitary internal waves (ISW). This ISW propagates from its formation in the sill not only in one direction but in various directions. The internal waves that are formed have three different propagation patterns: southward, northward, and both directions. This depends on ITF flow, water stratification and tidal conditions at the time the internal wave formation occurs (Susanto *et al*., 2005). In this study, it was observed that ISW was still strong enough to spread in the waters of the Bali Sea to touch the Kangean Islands. At the time of yo-yo CTD data collection, the distribution pattern of physical parameters (temperature, salinity and density) can still be seen quite clearly following the internal wave pattern, especially in the thermocline layer.

Conclusion

Bali Sea have the characteristics of well stratified seawaters which might be influenced by an internal tides coming from Lombok Strait. Identified 4 types of water masses in a row, from the surface there are Java Sea water masses, mixed water masses between Java Sea and ITF, NPSW and NPIW with modified water mass property characters. Vertical distribution the water mass follows stratification and there is no overlap between one type of water mass and another. High Brunt Vaisala values were found in the stable thermocline layer. This is in accordance with small variations of the Thorpe displacement in the thermocline layer. The estimation of turbulent mixing parameters obtained energy dissipation value of 1.58 x 10^{-9} W kg^{-1} and diapycnal diffusivity 5.07 x 10^{-5} m^2 s^{-1} which is equivalent to the open ocean. This proves the high value of localized mixing in certain areas. The value of turbulent mixing is found to be highest in the thermocline layer and decreases with increasing depth. Atmospheric dynamics represented by the wind at the time of yo-yo CTD data collection showed that the southeast monsoon winds moved to the southwest. The highest wind speed intensity is in the middle of the Indian Ocean. The surface current in the study area is dominant towards the south in accordance with the ITF direction and intensification occurs in the Lombok Strait due to the narrow bathymetry of the waters. It is clear that there is internal wave propagation during Yoyo CTD data collection as confirmation of the similar pattern

between the transverse profile of physical parameters and tidal elevation.

Acknowledgment

The author would like to thank PUSHIDROSAL who has carried out the expedition and allowed to process the data. The author also thanks the reviewers who have provided valuable reviews and improved the paper. Special thanks to Department of Marine Science and Technology Bogor Agriculture University for Sentinel 1 Image Processing in North Bali Sea.

References

Adhyatma, D., Atmadipoera, A.S., Naulita, Y., Nugroho, D. & Herlisman, 2019. Analysis of turbulent mixing in the Eastern Path of Indonesian Throughflow. *IOP Conf. Ser. Earth Environ. Sci.,* 278: 012003. doi: 10.1088/1755-1315/278/1/012003

Aiki, H., Matthews, J.P. & Lamb, K.G., 2011. Modeling and energetics of tidally generated wave trains in the Lombok Strait: impact of the Indonesian Throughflow. *J. Geophys. Res. Ocean*. 116(C3): 17p. doi: 10.1029/2010JC0 06589

Aldrian, E. & Susanto, R.D. 2003. Identification of three dominant rainfall regions within Indonesia and their relationship to sea surface temperature. *Int. J. Climatol.,* 23(12): 1435–1452. doi: 10.1002/joc.950.

Arief, D. & Murray, S.P. 1996. Low-frequency fluctuations in the Indonesian Throughflow through Lombok Strait. *J. Geophys. Res.,* 101(C5): 12455–12464. doi: 10.1029/96JC0 0051

Atmadipoera, A., Molcard, R., Madec, G., Wijffels, S., Sprintall, J., Koch-Larrouy, A., Jaya, I. & Supangat, A., 2009. Characteristics and variability of the Indonesian throughflow water at the outflow straits. *Deep. Res. Part I Oceanogr. Res. Pap.* 56: 1942–1954. doi: 10.1016/j.dsr. 2009.06.004.

Bouruet-Aubertot, P., Cuypers, Y., Ferron, B., Dausse, D., Ménage, O., Atmadipoera, A., Jaya, I., Olivier, M., Atmadipoera, A. & Jaya, I., 2018. Contrasted turbulence intensities in the Indonesian Throughflow: a challenge for parameterizing energy dissipation rate. *Ocean Dyn*., 68: 1–75. doi: 10.1007/s10236-018-11 59-3.

Crawford, W.R. 1986. A comparison of length scales and decay times of turbulence in stably stratified flows. *J. Phys. Oceanogr.,* 16: 1847–1854

Dillon, T.M. 1982. Vertikal overturns: a comparation of Thorpe and Ozmidov length scale. *J. Geophys. Res.* 87: 9601-9613

Emery, W.J. & Thomson, R.E. 1998. Data Analysis Method in Physical Oceanography. BPC Weatons, Britain, 634 p.

Fang, G., Susanto, R.D., Wirasantosa, S., Qiao, F., Supangat, A., Fan, B., Wei, Z., Sulistiyo, B. & Li, S. 2010. Volume, heat, and freshwater transports from the South China Sea to Indonesian Seas in the boreal winter of 2007–2008. *J. Geophys. Res.,* 115(C12): 17p doi: 10.10 29/2010JC006225.

Fieux, M., Andrie, C., Charriaud, E., Ilahude, A.G., Metzl, N., Molcard, R. & Swallow, J.C. 1996. Hydrological and chlorofluoromethane measurements of the Indonesian throughflow entering the Indian Ocean. *J. of Geophys. Res.*, 101(C5): 12433-12454.

Fine, R.A., Lukas, R., Bingham, F.M., Warner, M.J. & Gammon, R.H., 1994. The western equatorial Pacific: A water mass crossroads. *J. Geophys. Res.,* 99: 25063–25080. doi: 10.1029/94jc0 2277

Galbraith, P.S. & Kelley, E. 1996. Identifying overturn in CTD profiles. *J. Atmos. Ocean Tech*., 13: 688-702

Gordon, A.L., Sprintall, J., Van Aken, H.M., Susanto, D., Wijffels, S., Molcard, R., Ffield, A., Pranowo, W. & Wirasantosa, S. 2010. The Indonesian Throughflow during 2004–2006 as observed by the INSTANT Program. *Dyn. Atmospheres Oceans,* 50(2): 115–128, doi: 10.1016/j.dyna tmoce.2009.12.002.

Gordon, A.L. & Fine, R.A. 1996. Pathways of water between the Pacific and Indian Oceans in the Indonesian seas. *Nature*, 379(6561): 146–149, doi: 10.1038/379146a0.

Gregg, M.C. 1998. Estimation and geography of diapycnal mixing in the stratified ocean, *Coast. Estuar. Stud.,* 54: 305–338,

Guo, P., Fang, W., Gan, Z., Chen, R. & Long, X. 2006. Internal tide characteristics over northern South China Sea continental slope. *Chin. Sci. Bull.,* 51(2): 17-25. doi: 10.1007/s11434-006-9017-y

Hao. J,, Chen, Y., Wang, F. & Lin, P. 2012. Seasonal thermocline in the China Seas and northwestern Pacific Ocean. *J. Geophys. Res.,* 117: C02022

Hatayama, T. 2004. Transformation of the Indonesian throughflow water by vertical mixing and its relation to tidally generated internal waves. *J. Oceanogr.* 60: 569–585. doi: 10.1023/B:JOCE. 0000038350.32155.cb.

Karang, I.W.G.A., Nishio, F., Mitnik, L. & Osawa, T. 2012. Spatial-Temporal Distribution and Characteristics of Internal waves in the Lombok Strait Area Studied by Alos-Palsar Images. *Earth Sci. Res.,* 1(2): p11

Kashino, Y., Aoyama, M., Kawano, T., Hendiarti, N., Muneyama, K., Watanabe, H. & Sea, P., 1996. The water masses between Mindanao and New Guinea. *J. Geophys. Res.* 101: 2391–12400. doi: 10.1029/95JC03797

Koch-Larrouy, A., Lengaigne, M., Terray, P., Madec, G. & Masson, S., 2010. Tidal mixing in the Indonesian seas and its effect on the tropical climate system. *Clim. Dyn*. 34: 891–904. doi: 10.1007/s00382-009-0642-4.

Koch-Larrouy, A., Madec, G., Bouruet-Aubertot, P., Gerkema, T., Bessi`eres, L. & Molcard, R., 2007. On the transformation of Pacific Water into Indonesian Throughflow Water by internal tidal mixing. *Geophys. Res. Lett.* 34(4): 1-6 doi: 10.1029/2006GL028405

Ledwell, J.R., Montgomery, E.T., Polzin, K.L., St Laurent, L.C., Schmitt, R.W. & Toole, J.M. 2000. Evidence for enhanced mixing over rough topography in the abyssal ocean, *Nature,* 403: 179–182, doi: 10.1038/35003164,

Mayer, B. & Damm, P.E. 2012. The Makassar Strait throughflow and its jet. *J Geophys Res.* 117(C07020): 1-14. doi: 10.1029/2011JC00 7809.

McTaggart, K.E., Johnson, G.C., Johnson, M.C., Delahoyde, F.M. & Swift, J.H. 2010. Notes on CTD/O2 data acquisition and processing using Sea-Bird hardware and software (as available). *Go-Ship IOCCP Rep*. 14: 1-10

Molcard, R., Fieux, M. & Syamsudin, F. 2001. The throughflow within Ombai Strait. *Deep Sea Research Part I,* 48: 1,237–1,253, doi: 10.1016/S0967-0637(00)00084-4

Munk, W.H. 1966. Abyssal recipes. *Deep-Sea Res* 13: 707–730

Murray, S.P. & Arief, D. 1988. Throughflow into the Indian Ocean through Lombok Strait, January 1985-January 1986. *Nature.* 333: 444-447.

Nagai, T., Hibiya, T. & Syamsudin, F. 2021. Direct estimates of turbulent mixing in the Indonesian archipelago and its role in the transformation of the Indonesian throughflow waters. *Geophys Res Lett,* 48: e2020GL091731. doi: 1029/ 2020GL091731

Nagai, T. & Hibiya, T. 2015. Internal tides and associated vertical mixing in the Indonesian Archipelago. *J. Geophys. Res. C Ocean*. 120(5): 3373–3390. doi: 10.1002/2014JC010592.

Nagai, T., Hibiya, T. & Bouruet-Aubertot, P., 2017. Nonhydrostatic simulations of tide induced mixing in the Halmahera Sea: a possible role in the transformation of the Indonesian throughflow waters*. J. Geophys. Res. Ocean*. 122: 8933–8943. doi: 1002/2017JC013381

Nugroho, D., Koch-larrouy, A., Gaspar, P., Lyard, F., Re, G. & Tranchant, B., 2018. Modelling explicit tides in the Indonesian Seas: an important process for surface sea water properties. *Mar. Poll. Bull.* 131: 7-18. doi: 10.1016/j. marpolbul.2017.06. 033.

Osborn, T.R. 1980. Estimates of the local rate of vertical diffusion from dissipation measurements. *J. Phys. Oceanogr*., 10: 83–89

Polzin, K.L., Toole, J.M. & Schmitt, R.W. 1995. Finescale Parameterizations of Turbulent Dissipation, *J. Phys. Oceanogr.,* 25: 306–328, doi: 10.1175/1520

Pratomo, Y., Pranowo, W.S. & Setiadi, H., 2016. Identifikasi penjalaran gelombang panjang Samudera Hindia ke Selat Lombok berdasarkan komponen harmonik arus. *Omni-Akuatika,* 12(1): 22-29 doi: 10.20884/1.oa. 2016. 12.1.26.

Purwandana, A., Cuypers, Y. & Bouruet-Aubertot, P. 2021. Observation of internal tides, nonlinear internal waves and mixing in the Lombok Strait, Indonesia. *Cont. Shelf Res.,* 216: 104358. doi: 10.1016/j.csr.2021.104358.

Purwandana, A., Cuypers, Y., Bouruet-Aubertot, P., Nagai, T., Hibiya, T. & Atmadipoera, A.S. 2020. Spatial structure of turbulent mixing inferred from historical CTD datasets in the Indonesian seas. *Prog. Oceanogr.,* 184: 102312. doi: 10.1016/j.pocean.2020.102312

Purwandana, A., Purba, M., Atmadipoera, A.S., 2014. Distribusi percampuran turbulen di perairan selat alor. *Ilmu Kelautan : Indonesian Journal of Marine Science* 19: 43–54. doi: 10.14710/ ik.ijms.19.1.43-54

Ray, R.D. & Susanto, R.D. 2016. Tidal mixing signatures in the Indonesian seas from highresolution sea surface temperature data. *Geophys. Res. Lett.* 43: 8115–8123. doi: 10.1002/2016GL069485.

Robertson, R. & Ffield, A. 2005. M2 baroclinic tides in the Indonesian seas. *Oceanography* 18: 62–73. doi :10.5670/oceanog.2005.06

Schiller, A. 2004. Effects of explicit tidal forcing in an OGCM on the water-mass structure and circulation in the Indonesian throughflow region. *Ocean Model*. 6: 31–49. doi: 10.1016/S1463-5003(02)00057-4

Siregar, S.N., Sari, L.P., Purba, N.P., Pranowo, W.S. & Syamsuddin, M.L. 2017 Pertukaran Massa Air Di Laut Jawa Terhadap Periodisitas Monsun Dan Arlindo Pada Tahun 2015. *J. Ilmu-Ilmu Perairan, Pesisir dan Perikanan,* 6(1): 44-59, doi: 10.13170/depik.6.1.5523,

Sprintall, J., Gordon, A.L., Wijffels, S.E., Feng, M., Hu, S., Koch-Larrouy, A., Phillips, H., Nugroho, D., Napitu, A., Pujiana, K. & Susanto, R.D.. 2019. Detecting change in Indonesian seas. *Front. Mar. Sci.* 6: p257 doi: 10.3389/fmars.2019.00257

Sprintall, J., Wijffels, S., Gordon, A.L., Ffield, A., Molcard, R., Susanto, R.D., Soesilo, I., Sopaheluwakan, J., Surachman, Y. & van Aken, H.M. 2004. A new international array to measure the Indonesian Throughflow: INSTANT. *EOS, Transactions American Geophysical Union* 85(39): 369–376, doi: 10.1029/2004E0390002

Sprintall, J., Wijffels, S.E., Molcard, R. & Jaya, I. 2009. Direct estimates of the Indonesian Throughflow entering the Indian Ocean: 2004– 2006. *J. Geophys. Res.* 114(C7): 1-19 doi: 10.1029/2008JC005257

Stansfield, K., Garrett, C. & Dewey, R. 2001. The probability distribution of the Thorpe displacement within overturns in Juan de Fuca Strait. *J. Phys. Oceanogr*. 31: 3421- 3434.

Stewart, R.H. 2002. Introduction to Phys Oceanography. Texas A and M University. Department of Oceanography

Susanto, R.D., Mitnik, L. & Zheng, Q., 2005. Ocean Internal Waves Observed in the Lombok Strait. *Oceanography* 18(4): 80-87. doi: 10.5670/ocea nog.2005.08

Susanto, R.D. & Gordon, A.L. 2005. Velocity and transport of the Makassar Strait throughflow. *J. Geophy. Res.* 110(C1):1-10 doi: 10.1029/2004JC002425

Susanto, R.D. & Song, Y.T. 2015. Indonesian throughflow proxy from satellite altimeters and gravimeters. *J. Geophysical Res.* 120(4): 2844–2855, doi: 10.1002/2014JC01 0382

Susanto, R.D., Wei, Z., Adi, T.R., Zheng, Q., Fang, G., Fan, B., Supangat, A., Agustiadi, T., Li, S., Trenggono, M. & Setiawan, A. 2016. Oceanography surrounding Krakatau Volcano in the Sunda Strait, Indonesia. *Oceanography,* 29(2): 264–172. doi: 10.5670/oceanog.2016. 31

Suteja, Y., Purba, M. &Atmadipoera, A.S., 2015. Percampuran Turbulen di Selat Ombai. *J. Ilmu dan Teknol. Kelaut. Trop.* 7:71–82. doi: 10.29244/jitkt.v7i1.9778

Syamsudin, F., Taniguchi, N., Zhang, C., Hanifa, A.D., Li, G., Chen, M., Mutsuda, H., Zhu, Z.N., Zhu, X.H., Nagai, T. & Kaneko, A. 2019. Observing internal solitary waves in the Lombok Strait by coastal acoustic tomography. *Geophys Res Lett*., 46(17-18): 10475-10483

van Aken, H.M., Brodjonegoro, I. & Jaya, I. 2009. The deep-water motion through the Lifamatola Passage and its contribution to the Indonesian throughflow. *Deep Sea Research Part I* 56: 1203–1216, doi: 10.1016/j.dsr.2009.02.001.

Wang, J., Yuan, D., Li, X., Li, Y., Wang, Z., Hu, X., Zhao, X., Corvianawatie, C. & Surinati, D 2020. Moored observations of the Savu Strait currents in the Indonesian seas. *J. Geophys. Res.* 125(7): e2020JC016082, doi: 10.1029/2020JC016 082

Wang, Y., Xu, T., Li, S., Susanto, R.D., Agustiadi, T., Trenggono, M., Tan, W. & Wei, Z., 2019. Seasonal variation of the water transport through the Karimata Strait. *Acta Oceanologica Sinica,* 4: 47–57, doi: 10.1007/s13131-018-1224-2.

Wirasatriya, A., Setiawan, J.D., Sugianto, D.N., Rosyadi, I.A., Haryadi, H., Winarso, G., Setiawan, R.Y. & Susanto, R.D., 2020. Ekman dynamics variability along the southern coast of Java revealed by satellite data. *Int. J. Remote Sens.,* 41(21): 8,475–8,496, doi: 10.1080/01431161.2020.1797215

Wu, L. X., Jing, Z., Riser, S. & Visbeck, M. 2011. Seasonal and spatial variations of Southern Ocean diapycnal mixing from Argo profiling floats. *Nat. Geosci.,* 4: 363–366, doi: 10.1038/Ngeo1156

Wyrtki, K. 1987. Indonesian through flow and the associated pressure gradient. *J. Geophys. Res*., 92(C12): 12942–12946, doi: 10.1029/JC092iC12p12941.

Wyrtki, K., 1961. Physical oceanography of the Southeast Asian waters. Scientific Result as Mar. Investig. *South China Sea Gulf Thailand*., 2: 195. doi: 10.1017/S0025315400054370.

Yuliardi, A.Y., Atmadipoera, A.S., Harsono, G., N. Natih, N.M. & Ando, K. 2021. Analysis of Characteristics and Turbulent Mixing of Seawater Mass in Lombok Strait. *Ilmu Kelautan: Indonesian Journal of Marine Sciences,* 26(2): 95-109. doi: 10.14710/ik. ijms.26.2.95-109